Front. Chem. Sci. Eng. 2021, 15(5): 1197–1205
https://doi.org/10.1007/s11705-020-1998-6

RESEARCH ARTICLE

Kinetics and mechanism of nitrobenzene degradation by hydroxyl radicals-based ozonation process enhanced by high gravity technology

Weizhou Jiao (✉), Shengjuan Shao, Peizhen Yang, Kechang Gao, Youzhi Liu

Shanxi Province Key Laboratory of Higee-Oriented Chemical Engineering, National Demonstration Center for Experimental Comprehensive Chemical Engineering Education, North University of China, Taiyuan 030051, China

Abstract This study investigated the indirect oxidation of nitrobenzene (NB) by hydroxyl radicals (·OH) in a rotating packed bed (RPB) using competitive kinetics method with *p*-nitrochlorobenzene as a reference compound. The rate constants of NB with ·OH are calculated to be between $(1.465\pm0.113) \times 10^9$ L/(mol·s) and $(2.497\pm0.192) \times 10^9$ L/(mol·s). The experimental data are fitted by the modified Arrhenius equation, where the activation energy is 4877.74 J/mol, the order of NB concentration, rotation speed, and initial pH is 0.2425, 0.1400 and 0.0167, respectively. The ozonation process of NB could be enhanced by RPB, which is especially effective for highly concentrated NB-containing wastewater under alkaline conditions. The high gravity technology can accelerate ozone mass transfer and self-decomposition of ozone to produce more ·OH, resulting in an increase in the indirect oxidation rate of NB by ·OH and consequently effective degradation of NB in wastewater.

Keywords high gravity technology, hydroxyl radicals, nitrobenzene, reaction kinetics

1 Introduction

Nitrobenzene (NB) is an important chemical raw material used in industrial production of dyes, explosives, pesticides and medicines [1,2]. It is estimated that approximately 10000 tons of NB-containing wastewater is discharged into the environment each year [3], which can have significant ecological and health consequences due to the carcinogenic, teratogenic and mutagenic effects of NB [4,5]. However, the substituted nitro group of NB makes it difficult to be completely degraded by traditional biological and chemical methods [6]. Now, NB has been listed as a priority pollutant by the US Environmental Protection Agency and the Ministry of Environmental Protection of China [7]. Therefore, it is very important to find an economical and efficient method for the degradation of NB compounds in water.

Advanced oxidation processes (AOPs) such as O_3/H_2O_2, UV/O_3, UV/H_2O_2/O_3 and O_3/catalyst have proven to be effective methods for the removal of toxic and bio-resistant organic compounds due to the high oxidation capacity of O_3 ($E^\theta = 2.07$ V) [3,8–10]. It is also known that O_3 can oxidize organic compounds through the direct oxidation by dissolved ozone or the indirect oxidation by ·OH ($E^\theta = 2.80$ V) decomposed from the dissolved ozone in water [11,12]. Previous studies have shown that the direct reaction rate constant of O_3 with NB was extremely low (0.09–2.2 L/(mol·s)) in the batch reactor under low pH [13,14]. Given that ·OH can non-selectively and rapidly oxidize pollutants with a reaction rate in the range of 10^8–10^{10} L/(mol·s) [15], attempts have been made to enhance the indirect oxidation by promoting the self-decomposition of ozone into ·OH.

The performance of the ozonation system can be impaired by the low gas-liquid mass transfer rate due to poor water solubility of O_3, while the gas-liquid mixing and reaction can be enhanced with the use of a rotating packed bed (RPB). In the RPB, the gravity force (g) is replaced with a centrifugal force up to several hundreds folds of g, so that the liquid flows as filaments, thin films or tiny droplets [16] and the liquid volumetric mass transfer coefficient (k_La) could be 2–8 times higher than that in a

Received May 3, 2020; accepted July 25, 2020

E-mail: jwz0306@126.com

conventional reactor [17–19]. Thus, the high gravity technology in combination with ozonation can significantly improve the degradation efficacy of organic pollutants in wastewater.

Zeng et al. [20] investigated the degradation of phenol using O_3/Fenton in RPB, and the results showed that the BOD_5/COD (0.58) in RPB was much higher than that in the stirred tank reactor (0.43), and increasing the rotor speed of RPB from 300 to 1500 r/min caused an increase of k_La from 0.036 to 0.875 s^{-1}. Jiao et al. [21] investigated the degradation of NB-containing wastewater with O_3 and H_2O_2 in RPB, and the high mass transfer in RPB resulted in an increase in the removal rate of NB and COD by 23.3% and 22.9% compared with that of conventional aeration methods, respectively. Guo et al. [22] showed that RPB-O_3/H_2O_2 has achieved a removal efficiency of 90% for NB after 25 min at an initial concentration of 200 mg/L, which was 30% higher than that in the conventional bubbling reactor.

The enhanced ozonation efficiency of high gravity technology may result from the intensified ozone mass transfer, especially for pollutants with high reaction rates with ozone. RPB presents a turbulent regime, which could increase the collision frequency between aqueous ozone and hydroxide ions in water, and thus lead to enhanced decomposition of aqueous ozone into ·OH. It is proved that the generation of ·OH from ozone decomposition is significantly affected by temperature, hydroxide ions, gaseous ozone concentration, coexisting substances, and degree of liquid turbulence [23–25]. Our group compared the decomposition rate of ozone in the traditional magnetic stirrer and RPB under similar experimental conditions, and the results showed that at the same rotor speed, the apparent rate constant of ozone decomposition was 1.58×10^{-3} s^{-1} in the RPB, which was higher than that in the traditional magnetic stirrer (1.43×10^{-3} s^{-1}). The half-life of O_3 in boiled deionized water was 93 s in the RPB but 393 s in the conventional magnetic stirrer [23]. An important advantage of the high gravity technology is that the high-speed rotating packing could increase the liquid turbulence, surface film renewal and specific interfacial area, which is beneficial to the decomposition of ozone into ·OH. An increase of ·OH exposure will increase the indirect oxidation by ·OH.

Our previous work has shown that the reaction rate constants of the direct oxidation of NB by O_3 in the RPB vary from 0.732 to 5.267 L/(mol·s) [3], but the direct oxidation of NB by O_3 under low pH showed slow kinetics. This study investigated the enhanced indirect oxidation kinetics of NB by ·OH in the RPB due to the improved mass transfer and accelerated ozone self-decomposition. The reaction rate constants of ·OH and NB under high gravity were determined, and an empirical model was established.

2 Experimental

2.1 Experimental process

The NB solutions of different concentrations (100–500 mg/L) were prepared by dissolving NB in deionized water in a 2.0 L volumetric flask at room temperature, and *p*-chloronitrobenzene (*p*-CNB) powder was dissolved in deionized water to obtain the concentration required for each run. A cross-flow rotating packed bed with wire mesh is used in this study, where the inner radius is 4.0 cm, the outer radius is 7.5 cm, the packing height is 7.5 cm, and the specific surface area of the wire-mesh packing is 935.07 m^2/m^3 with a void of 0.74. As seen in Fig. 1, the aqueous solution containing NB was continuously pumped into the inner side of the RPB via a liquid distributor and then thrown outward through the packing under high centrifugal force. The solution was then recycled to the storage tank for the next run. The gaseous ozone with O_2 flowed upward vertically from the bottom of the RPB. The cross-flow contact between the liquid and gas in the packing allowed for effective mass transfer, and subsequently the competitive oxidation reactions of NB and *p*-CNB by ·OH.

In the previous study, experiments were conducted under low pH in the presence of *t*-BuOH in order to avoid the impacts of indirect oxidation. In this case, ozone is hardly decomposed into ·OH, and thus the degradation of NB can be ascribed to the direct oxidation by ozone. In this study, experiments were conducted under high pH in order to elucidate the indirect oxidation of NB by ·OH [26].

2.2 Analytical methods

The NB and *p*-CNB solutions were analyzed by high-performance liquid chromatography (HPLC; Ultimate 3000, Thermo Fisher Scientic, USA) on a C18 reversed phase column, where the detection wavelength was 262 nm and 220 nm, the methanol-water (70:30) acted as mobile phases with a flow rate of 0.9 mL/min and the column temperature was 20 °C. The gaseous ozone concentration was determined by an ozone concentration detector (UV-2200C, China).

2.3 Kinetic model

Both indirect and direct oxidation would occur during ozonation. The overall reaction rate constant k_O can be calculated by Eqs. (1–4), where R_{ct} is supposed to be a constant (the concentration ratio of ·OH-exposure and O_3-exposure) [27].

$$-\frac{d[NB]}{dt} = k_{O_3,NB}[NB][O_3] + k_{\cdot OH,NB}[NB][\cdot OH], \quad (1)$$

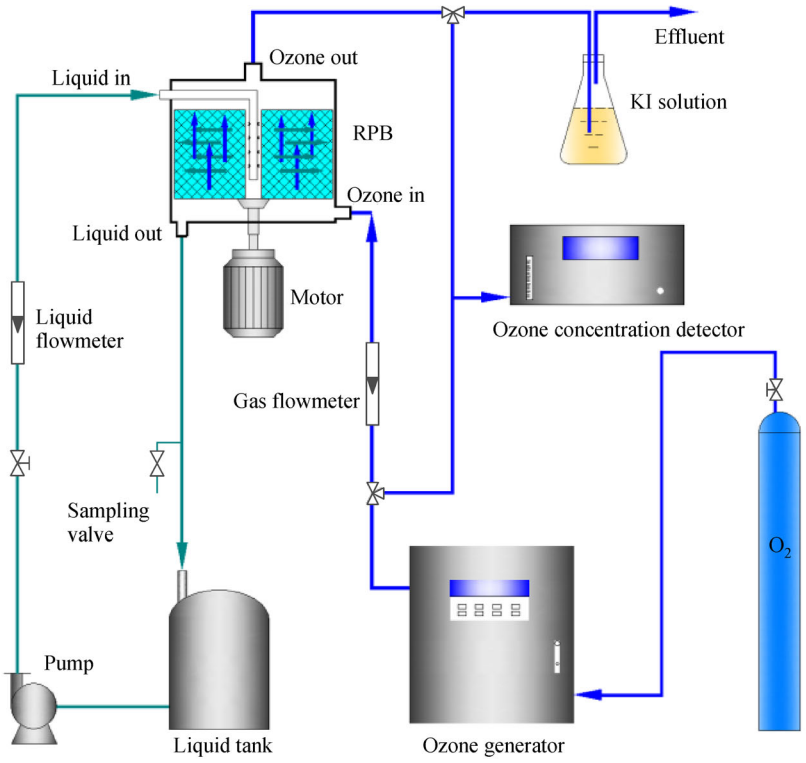

Fig. 1 Flow chart of the ozonation process in the RPB.

$$-\frac{\mathrm{d}[\mathrm{NB}]}{\mathrm{d}t} = (k_{\mathrm{O_3,NB}} + k_{\cdot\mathrm{OH,NB}}R_{\mathrm{ct}})[\mathrm{NB}][\mathrm{O_3}]$$

$$= k_{\mathrm{O}}[\mathrm{NB}][\mathrm{O_3}], \quad (2)$$

$$-\ln\frac{C_{\mathrm{NB},t}}{C_{\mathrm{NB},0}} = k_{\mathrm{O}}\int_0^t [\mathrm{O_3}]\mathrm{d}t, \quad (3)$$

$$k_{\mathrm{O}} = k_{\mathrm{O_3,NB}} + k_{\cdot\mathrm{OH,NB}}R_{\mathrm{ct}}, \quad (4)$$

$$R_{\mathrm{ct}} = \int_0^t [\cdot\mathrm{OH}]\mathrm{d}t \Big/ \int_0^t [\mathrm{O_3}]\mathrm{d}t. \quad (5)$$

For direct oxidation, $k_{\mathrm{O_3,NB}}$ can be obtained directly by monitoring chemical decay over time regardless of the exposure of ·OH. However, as the reactions of ·OH with chemicals are often non-selective with fast reaction rates, it is very difficult to directly determine the reaction rate constants of ·OH with NB. The competition kinetics method is recommended to determine the indirect rate constants of organics with ·OH that are higher than 10^4 L/(mol·s) [28]. Leitner et al. [29] determined the rate constants of ·OH with benzotriazole using the competition kinetics method with ibuprofen and diuron as reference compounds, and found that benzotriazole showed a high reactivity toward ·OH in a wide range of pH and these highly reactive species could contribute to the oxidation of benzotriazole during ozonation. El Najjar et al. [30] carried out ozonation experiments using the competition kinetics method with carbamazepin as a competitor and developed a model to predict the removal of levofloxacin based on the R_{ct} concept. Wang et al. [31] also used the competition kinetics method to determine the reaction rate constants between dibutyl phthalate (DBP) and ·OH and SO_4^{-}· with *p*-chloronitrobenzene (*p*-CNB) as the reference, and found that the pseudo-first-order rate constant was significantly affected by the initial DBP concentration, solution pH and coexisting ions or inhibitors.

In order to determine the indirect reaction kinetics, *p*-CNB with a reaction rate constant of $(2.6\pm0.2) \times 10^9$ L/(mol·s) with ·OH but only 1.6 L/(mol·s) with O_3 was used as a competing compound [32,33]. The relative decay rate of NB to the competing compound (*p*-CNB) can be expressed as follows according to Eqs. (1–4):

$$\ln\left(\frac{C_{p\text{-CNB},0}}{C_{p\text{-CNB},t}}\right)\Big/\ln\left(\frac{C_{\mathrm{NB},0}}{C_{\mathrm{NB},t}}\right)$$

$$= (k_{\cdot\mathrm{OH},p\text{-CNB}}R_{\mathrm{ct}} + k_{\mathrm{O_3},p\text{-CNB}})$$

$$/(k_{\cdot\mathrm{OH,NB}}R_{\mathrm{ct}} + k_{\mathrm{O_3,NB}}). \quad (6)$$

As the values of $k_{\mathrm{O_3,NB}}$ and $k_{\mathrm{O_3},p\text{-CNB}}$ are negligibly small, Eq. (6) can be simplified into:

$$\ln\left(\frac{C_{\mathrm{NB},0}}{C_{\mathrm{NB},t}}\right)\Big/\ln\left(\frac{C_{p\text{-CNB},0}}{C_{p\text{-CNB},t}}\right)=k_{\cdot\mathrm{OH,NB}}/k_{\cdot\mathrm{OH},p\text{-CNB}}. \quad (7)$$

$k_{\cdot\mathrm{OH,NB}}$ can be calculated as follows:

$$k_{\cdot\mathrm{OH,NB}}=\frac{\ln(C_{\mathrm{NB},0}/C_{\mathrm{NB},t})}{\ln(C_{p\text{-CNB},0}/C_{p\text{-CNB},t})}\times k_{\cdot\mathrm{OH},p\text{-CNB}}, \quad (8)$$

where $C_{\mathrm{NB},0}$ and $C_{p\text{-CNB},0}$ are the initial concentrations of NB and *p*-CNB, mg/L; $C_{\mathrm{NB},t}$ and $C_{p\text{-CNB},t}$ are the concentrations of NB and *p*-CNB at time *t*, mg/L; and $k_{\cdot\mathrm{OH,NB}}$ and $k_{\cdot\mathrm{OH},p\text{-CNB}}$ are the rate constants for the reaction of ·OH with NB and *p*-CNB, L/(mol·s), respectively. As the initial NB concentration changes, $\ln(C_{p\text{-CNB},0}/C_{p\text{-CNB},t})$ as a function of $\ln(C_{\mathrm{NB},0}/C_{\mathrm{NB},t})$ can be plotted, and $k_{\cdot\mathrm{OH,NB}}$ value can be obtained by multiplying the inverse of $\ln(C_{p\text{-CNB},0}/C_{p\text{-CNB},t})/\ln(C_{\mathrm{NB},0}/C_{\mathrm{NB},t})$ by $k_{\cdot\mathrm{OH},p\text{-CNB}}$ value.

3 Results and discussion

The rate constants determined under alkaline conditions follow the order of $k_{\cdot\mathrm{OH,NB}}\times R_{\mathrm{ct}}>>k_{\mathrm{O_3,NB}}$. The dominant reaction is the indirect reaction of ·OH with organics, while the oxidation effect of O_3 can be neglected [32]. Experiments were conducted at a liquid flow rate V_{L} of 100 L/h and a gas flow rate Q_{G} of 75 L/h, and the effects of different parameters (temperature *T*, initial pH, initial NB concentration C_{NB}, and rotor speed *N*) on the rate constant $k_{\cdot\mathrm{OH,NB}}$ between NB and ·OH were investigated.

3.1 Effect of temperature on $k_{\cdot\mathrm{OH,NB}}$

Our previous work has revealed that temperature has a significant impact on the direct oxidation of NB [3]. Figure 2 shows that as temperature increases from 293 K to 313 K, the value of $k_{\cdot\mathrm{OH,NB}}$ is increased by 15.1% from (1.898±0.145) ×10^9 to (2.184±0.168) ×10^9 L/(mol·s). However, further increase of temperature only leads to a 9.2% increase in the value of $k_{\cdot\mathrm{OH,NB}}$. The main reason is that the self-decomposition of aqueous ozone is slow at pH < 12, which is a rate-limiting step for the indirect oxidation of NB by ·OH. As temperature increases, the intrinsic reaction rate constant of NB oxidation increases according to the Arrhenius equation. The self-decomposition rate of aqueous ozone is also increased with increasing temperature, resulting in an increase in the indirect reaction rate [24]. However, both volumetric mass-transfer coefficient and saturation concentration of ozone decrease as temperature increases [3], which may inhibit the increase in the intrinsic reaction rate constant. Therefore, the effects of temperature on the indirect oxidation of NB and mass transfer of ozone are mutually antagonistic. Since the mass-transfer rate and saturation concentration of ozone are decreased at high temperatures, which is not favorable for the formation of ·OH and the indirect oxidation of NB, the temperature should not be too high due to the negative effects on the mass transfer of ozone.

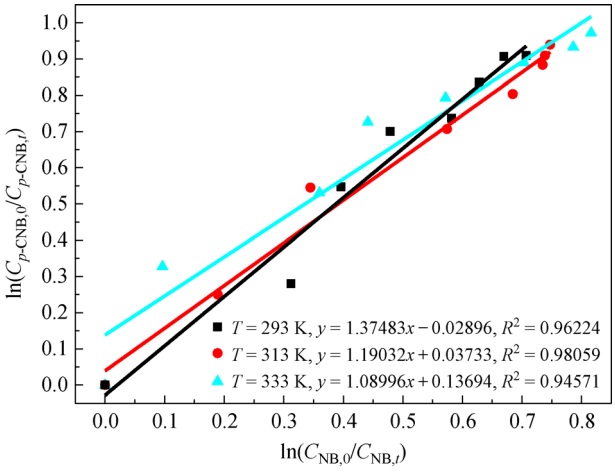

Fig. 2 Effect of temperature on $k_{\cdot\mathrm{OH,NB}}$. pH = 11.0, *N* = 700 r/min, $C_{\mathrm{NB}}=C_{p\text{-CNB}}$ = 200 mg/L, $C_{\mathrm{O_3}}$ = 40 mg/L, V_{L} = 100 L/h, Q_{G} = 75 L/h; *T* = 293 K, $k_{\cdot\mathrm{OH,NB}}$ = (1.898±0.145) × 10^9 L/(mol·s), *T* = 313 K, $k_{\cdot\mathrm{OH,NB}}$ = (2.184±0.168) × 10^9 L/(mol·s); *T* = 333 K, $k_{\cdot\mathrm{OH,NB}}$ = (2.385±0.183) × 10^9 L/(mol·s).

3.2 Effect of initial solution pH on $k_{\cdot\mathrm{OH,NB}}$

The solution pH is also an important factor affecting the indirect oxidation of organic pollutants, which is mainly attributed to its effect on the formation of ·OH, a typical chain initiator of ozone decomposition. The decomposition of aqueous ozone can be described as follows [24]:

Chain initiation reaction:

$$O_3 + OH^- \rightarrow HO_2^- + O_2 \quad (9)$$

$$O_3 + HO_2^- \rightarrow \cdot HO_2 + \cdot O_3^- \quad (10)$$

$$\cdot HO_2 \leftrightarrow O_2^- \cdot + H^+ \quad (11)$$

$$O_2^- \cdot + H^+ \rightarrow HO_2 \cdot \quad (12)$$

$$O_3 + \cdot O_2^- \rightarrow \cdot O_3^- + O_2 \quad (13)$$

Chain propagation reaction:

$$O_3^- \cdot + H_2O \rightarrow \cdot OH + O_2 + OH^- \quad (14)$$

$$O_3^- \cdot + \cdot OH \rightarrow \cdot HO_2 + \cdot O_2^- \quad (15)$$

$$O_3 + \cdot OH \rightarrow HO_4 \cdot \quad (16)$$

$$O_3^- \cdot + \cdot OH \rightarrow O_3 + OH^- \quad (17)$$

Chain termination reaction:

$$O_3 + CO_3^- \cdot \longrightarrow CO_2 + O_2 + O_2^- \cdot \quad (18)$$

$$HO_2^- + H_2O \longrightarrow H_2O_2 + OH^- \quad (19)$$

Thus, OH^- can initiate the decomposition chain reaction of O_3, as the main agent in water under high pH conditions. Figure 3 shows an obvious increase of $k_{\cdot OH,NB}$ from (1.465 ±0.113)×10^9 to (1.857±0.143)×10^9 L/(mol·s) as the initial solution pH increases from 7.0 to 11.0. However, further increase of the initial pH to 13.0 results in no changes in the reaction rates. That is because the OH^- concentration will increase with increasing initial pH, which can catalyze the decomposition of O_3 to form ·OH and thus result in an increase in $k_{\cdot OH,NB}$. However, this does not necessarily mean that a high initial pH is required, because collision of ·OH is more likely to occur at high pH. As a result, quenching reaction may occur and more ·OH will be consumed [34]:

$$\cdot OH + \cdot OH \longrightarrow H_2O_2 \quad (20)$$

Beltrán et al. showed that ·OH could reach an equilibrium with atomic oxygen radical anions at high pH [13]:

$$\cdot OH \leftrightarrow \cdot O^- + H^+, \quad pKa = 11.9 \quad (21)$$

The equilibrium moves rightward at an initial pH > 11.9, resulting in a decrease in the ·OH concentration. This is not favorable for the indirect reaction. Thus, the optimal initial pH is set to pH = 11.0 in this study.

3.3 Effect of rotor speed on $k_{\cdot OH,NB}$

Figure 4 shows that as the rotor speed increases from 300 to 900 r/min, the value of $k_{\cdot OH,NB}$ varies from (1.713±0.132) × 10^9 to (1.915±0.148) × 10^9 L/(mol·s), indicating that the indirect reaction rate constant can be improved by increasing the rotor speed. Both volumetric mass-transfer coefficient and saturation concentration of ozone would increase as the rotor speed increases [3,23], resulting in enhanced decomposition of aqueous ozone to ·OH and improved indirect oxidation of NB by ·OH. Our previous study has shown that the decomposition rate constant of ozone (k_d = 3.32 ×$10^{-5}N^{0.564}$) was dependent on the rotor speed within 0–900 r/min [23]. Thus, a high rotor speed is favorable for the decomposition of ozone into ·OH. Given that the rate-limiting step of the indirect oxidation is the self-decomposition of aqueous ozone, the strong turbulence regime of RPB is beneficial for the decomposition of ozone and thus favors the indirect reaction of NB and·OH. Specifically, the increase of rotor speed results in a higher increase in the mass transfer rate coefficient than the intrinsic reaction rate constant, which in turn results in increased exposure of ozone and ·OH and consequently improved degradation of NB [35]. In conclusion, there is a good contact between gas and liquid phases and an increase in the turbulence of solution in the RPB, which results in the enhanced mass transfer and self-decomposition of ozone, and consequently an increase in indirect oxidation efficiency of NB. However, the retention time of liquid in the packing can be reduced at high rotor speeds, which has a negative effect on the mass transfer of ozone [36]. Moreover, the energy consumption at high rotor speeds should also be taken into consideration [6].

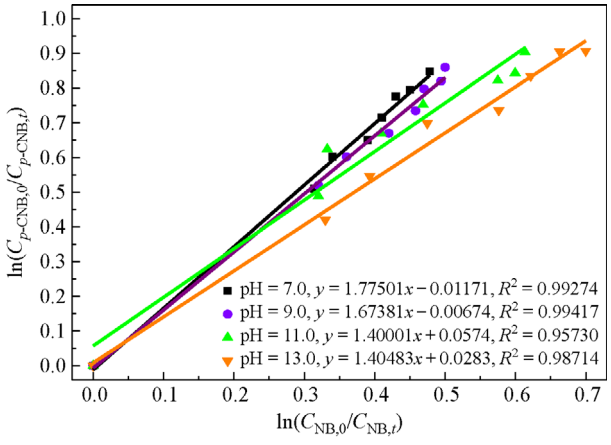

Fig. 3 Effect of initial solution pH on $k_{\cdot OH,NB}$. T = 293 K, N = 700 r/min, C_{NB} = $C_{p\text{-}CNB}$ = 200 mg/L, C_{O_3} = 40 mg/L, V_L = 100 L/h, Q_G = 75 L/h; pH = 7.0, $k_{\cdot OH,NB}$ = (1.465±0.113) × 10^9 L/(mol·s), pH = 9.0, $k_{\cdot OH,NB}$ = (1.553±0.119) × 10^9 L/(mol·s); pH = 11.0, $k_{\cdot OH,NB}$ = (1.857±0.143) × 10^9 L/(mol·s), pH = 13.0, $k_{\cdot OH,NB}$ = (1.851±0.145) × 10^9 L/(mol·s).

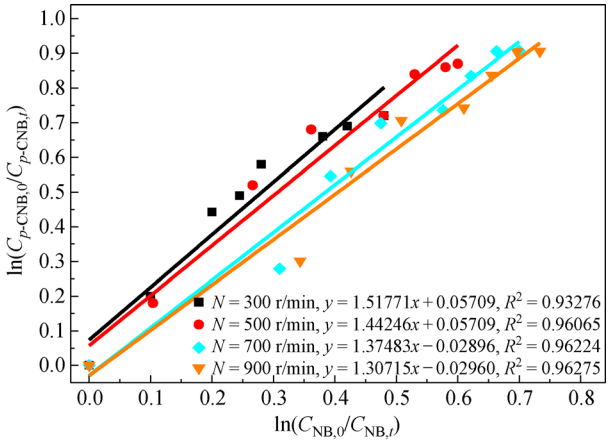

Fig. 4 Effect of rotor speed on $k_{\cdot OH,NB}$. T = 293 K, pH = 11.0, C_{NB} = $C_{p\text{-}CNB}$ = 200 mg/L, C_{O_3} = 40 mg/L, V_L = 100 L/h, Q_G = 75 L/h; N = 300 r/min, $k_{\cdot OH,NB}$ = (1.713±0.132) × 10^9 L/(mol·s), N = 500 r/min, $k_{\cdot OH,NB}$ = (1.802±0.139) × 10^9 L/(mol·s); N = 700 r/min, $k_{\cdot OH,NB}$ = (1.898±0.145) × 10^9 L/(mol·s), N = 900 r/min, $k_{\cdot OH,NB}$ = (1.915±0.148) × 10^9 L/(mol·s).

3.4 Effect of initial NB concentration on $k_{\cdot OH,NB}$

The $\ln(C_{p\text{-}CNB,0}/C_{p\text{-}CNB,t})$ as a function of $\ln(C_{NB,0}/C_{NB,t})$ is shown in Fig. 5. The value of $k_{\cdot OH,NB}$ is increased by 29.9% from $(1.735\pm0.134)\times10^9$ to $(2.254\pm0.173)\times10^9$ L/(mol·s) with the increase of C_{NB} from 100 to 300 mg/L. However, further increase of C_{NB} to 500 mg/L results in a 10.8% increment of $k_{\cdot OH,NB}$. At low concentrations, increasing the initial NB concentration can significantly promote the reaction rate constant according to the collision theory, whereas further increase of C_{NB} in the range of 300–500 mg/L seems to have no effect as few ·OH is obtained from the decomposition of aqueous ozone at a given O_3 dose, especially for a mass transfer controlled reaction.

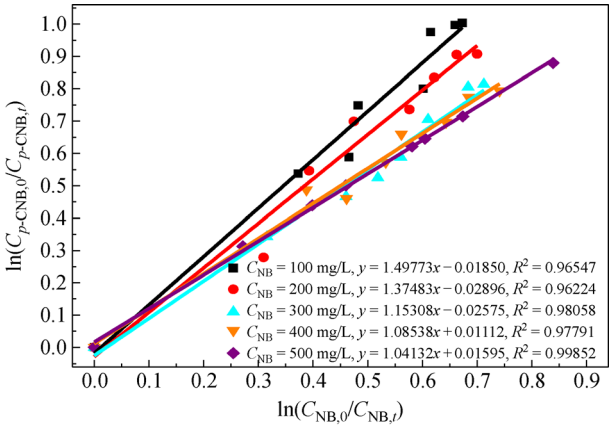

Fig. 5 Effect of initial NB concentration on $k_{\cdot OH,NB}$. T = 293 K, pH = 11.0, N = 700 r/min, C_{O_3} = 40 mg/L, V_L = 100 L/h, Q_G = 75 L/h; $C_{NB} = C_{p\text{-}CNB}$ = 100 mg/L, $k_{\cdot OH,NB} = (1.735\pm0.134)\times10^9$ L/(mol·s); $C_{NB} = C_{p\text{-}CNB}$ = 200 mg/L, $k_{\cdot OH,NB} = (1.898\pm0.145)\times10^9$ L/(mol·s); $C_{NB} = C_{p\text{-}CNB}$ = 300 mg/L, $k_{\cdot OH,NB} = (2.254\pm0.173)\times10^9$ L/(mol·s); $C_{NB} = C_{p\text{-}CNB}$ = 400 mg/L, $k_{\cdot OH,NB} = (2.395\pm0.184)\times10^9$ L/(mol·s); $C_{NB} = C_{p\text{-}CNB}$ = 500 mg/L, $k_{\cdot OH,NB} = (2.497\pm0.192)\times10^9$ L/(mol·s).

3.5 Reaction kinetic model

In order to better understand the effects of various factors, such as temperature, concentration, pH and catalyst on the reaction rate of the ozonation process, the experimental data are fitted by the modified Arrhenius equation [37,38]. Zhao et al. [38] fitted the overall oxidation rate of Red X-GRL with Arrhenius equation by the expression:

$$k_O = 108.013\exp\left(\frac{-15.298}{RT}\right)C_{OH^-}^{0.0037}. \quad (22)$$

Since the indirect oxidation rate constant of NB by ·OH is affected by temperature T, initial pH, rotor speed N and C_{NB}, the $k_{\cdot OH,NB}$ correlated to each operational parameter can be expressed by the modified Arrhenius equation as follows:

$$k_{\cdot OH,NB} = A\exp(-E_a/RT)C_{NB}^n C_{OH^-}^p N^q. \quad (23)$$

It can be transformed into:

$$\ln k_{\cdot OH,NB} = \ln A - E_a/RT + n\ln C_{NB} + p\ln C_{OH^-} + q\ln N, \quad (24)$$

where A is the pre-exponential factor; E_a is the reaction activation energy, J/mol; C_{OH^-} is the concentration of OH^- in water, mol/L; and n, p and q are the reaction order of C_{NB}, C_{OH^-}, and N, respectively. These parameters can be obtained by fitting $\ln k_{\cdot OH,NB}$ with each factor. 1) The curves of $\ln k_{\cdot OH,NB}$ against $1/T$ and $\ln C_{OH^-}$ (Fig. 6). The function of $\ln k_{\cdot OH,NB}$ against $1/T$ is described by the black line, where the slope equals to –586.69 (i.e., $-E_a/R$), and the activation energy E_a = 4877.74 J/mol. The function of $\ln k_{\cdot OH,NB}$ against $\ln C_{OH^-}$ is described as the red line with a slope of 0.0167 and a correlation coefficient R^2 of 0.9488. 2) The curves of $\ln k_{\cdot OH,NB}$ against $\ln N$ and $\ln C_{NB}$ (Fig. 7). The function of $\ln k_{\cdot OH,NB}$ against $\ln N$ is shown as the red line, where the slope equals to 0.14 and the correlation coefficient R^2 equals to 0.9971. The function of $\ln k_{\cdot OH,NB}$ against $\ln C_{NB}$ is shown as the black line with a slope of 0.2425 and a correlation coefficient R^2 of 0.9485. Finally, the A value is calculated to be 7.85×10^7 by substituting four sets of data into the equation and the $k_{\cdot OH,NB}$ could be given as follows:

$$k_{\cdot OH,NB} = 7.85\times10^7\exp(-4877.74/RT)C_{NB}^{0.2425}N^{0.1400}C_{OH^-}^{0.0167}. \quad (25)$$

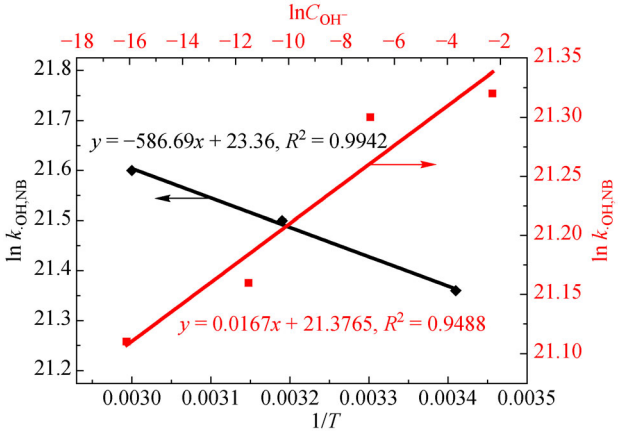

Fig. 6 The curves of $\ln k_{\cdot OH,NB}$ against $1/T$ and $\ln C_{OH^-}$.

Apparently, the indirect oxidation efficacy of NB by hydroxyl group is most affected by initial NB concentration, followed by rotor speed and solution pH. The E_a value is found to be significantly lower than the activation energy of 37431 J/mol for the direct oxidation of NB by ozone [3], indicating that the indirect oxidation is very

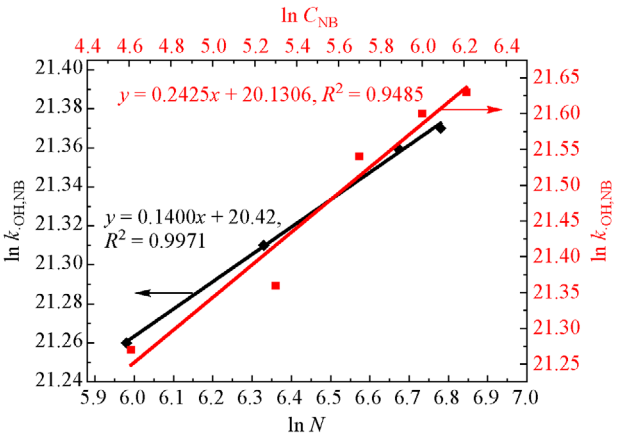

Fig. 7 The curves of ln $k_{\cdot OH,NB}$ against ln N and ln C_{NB}.

reactive and plays a dominant role in the advanced ozonation processes.

3.6 Comparison between direct and indirect reaction kinetic models

The reaction rate constant of the indirect oxidation is much higher than that of the direct oxidation, which prompts us to use advanced oxidation processes such as O_3/H_2O_2, O_3/Fenton and catalytic ozonation to enhance the indirect oxidation. In the RPB, the direct reaction rate constants are increased to 0.732–5.267 L/(mol·s), which are 2.4–8 times that of the traditional batch reactors [3,13,14]. Nevertheless, the direct oxidation of NB by ozone is still in the slow kinetic region. The indirect reaction rate constants are about $(1.465\pm0.113) \times 10^9$–$(2.497\pm0.192) \times 10^9$ L/(mol·s), which are 1.8–3 times that obtained by Matthews et al. (0.82×10^9 L/(mol·s)) [39]. This may be related to the experimental setups, reaction conditions and analytical methods. The self-decomposition rate of ozone is relatively slow at pH < 12, and the indirect reaction of NB and ·OH follows slow kinetics like the direct reaction. The oxidation pathway of NB is the combination of direct and indirect oxidation pathways. Comparison of the direct and indirect kinetic models shows that the reaction rate constant is 0.1498 and 0.14 order with respect to the rotor speed respectively, implying that RPB has almost the same effects on the direct and indirect reactions. In high pH solutions, the decomposition rate constants of ozone can be greater than 0.03–0.6 s^{-1} and the self-decomposition of ozone is in the rapid kinetics region [40]. Thus the rate-limiting step is the mass transfer of ozone, and the indirect reaction of ·OH with NB can be easily intensified in the RPB due to the improvement of ozone mass transfer. Thus, RPB is an ideal reactor for the ozonation process with high direct and indirect reaction rate constants. This is mainly attributed to the increased exposure of ozone and ·OH, and consequently increased occurrence of indirect oxidation, due to the improved mass transfer and self-decomposition of ozone. The enhanced ozonation process by RPB is especially effective for the treatment of highly concentrated NB-containing wastewater under alkaline conditions. Table 1 shows rate constants for direct and indirect reactions of NB with O_3 and ·OH.

4 Conclusions

In this study, the indirect oxidation kinetics of NB by ·OH in the RPB and the effects of different parameters on $k_{\cdot OH,NB}$ were investigated to uncover the enhanced ozonation mechanism by high gravity technology using the competitive kinetics method. The rate constants of NB with ·OH are calculated to be between $(1.465\pm0.113) \times 10^9$ L/(mol·s) and $(2.497\pm0.192) \times 10^9$ L/(mol·s) and the activation energy is significantly lower than that of the direct oxidation by ozone, indicating that indirect oxidation is very reactive for the oxidation of refractory organics. An empirical dynamic model is established, and the indirect oxidtaion kinetics of NB in the RPB are summarized. The high gravity technology can significantly increase the value of $k_{\cdot OH,NB}$ due to improved mass transfer and self-decomposition of ozone. The enhanced

Table 1 Rate constants for direct and indirect reactions of NB with O_3 and ·OH

Rate constant	Number	pH	Temperature/°C	Reference
$k_{O_3,NB}$/(L·mol^{-1}·s^{-1})				
(1.8±0.2)–(2.2±0.2)	1	2.0	10–20	Beltrán [13]
0.09±0.02	2	2.0	21–25	Hoigné [14]
0.732 – 5.261	3	1.0–7.0	20–60	This study
$k_{\cdot OH,NB} \times 10^{-9}$/(L·mol^{-1}·s^{-1})				
2.2	4	10.5	22–25	Hoigné [41]
0.82±0.3	5	10.5	18–25	Matthews [39]
(1.465±0.113)–(2.497±0.192)	6	7.0–13.0	20–60	This study

ozonation process by RPB is especially effective for the treatment of highly concentrated NB-containing wastewater under alkaline conditions.

Acknowledgements This work was supported by the Specialized Research Fund for Sanjin Scholars Program of Shanxi Province (No. 201707), Key Research & Development Plan of Shanxi Province (No. 201903D321059), Shanxi Scholarship Council of China (No. HGKY2019071), and Transformation and Cultivation Projects of Scientific and Technological Achievements of Higher Education Institutions for Shanxi Province (No. 2020CG040).

References

1. Liu H T, Sui M H, Yuan B J, Wang J Y, Lv Y N. Efficient degradation of nitrobenzene by Cu-Co-Fe-LDH catalyzed peroxymonosulfate to produce hydroxyl radicals. Chemical Engineering Journal, 2019, 357: 140–149
2. Palmisano G, Loddo V, Augugliaro V, Palmisano L, Yurdakal S. Photocatalytic oxidation of nitrobenzene and phenylamine: pathways and kinetics. AIChE Journal. American Institute of Chemical Engineers, 2010, 53: 961–968
3. Jiao W Z, Yang P Z, Gao W Q, Qiao J J, Liu Y Z. Apparent kinetics of the ozone oxidation of nitrobenzene in aqueous solution enhanced by high gravity technology. Chemical Engineering and Processing-Process Intensification, 2019, 146: 107690
4. Jiao W Z, Qin Y J, Luo S, He Z, Feng Z R, Liu Y Z. Simultaneous formation of nanoscale zero-valent iron and degradation of nitrobenzene in wastewater in an impinging stream-rotating packed bed reactor. Chemical Engineering Journal, 2017, 321: 564–571
5. Duan H T, Liu Y, Yin X H, Bai J F, Qi J. Degradation of nitrobenzene by Fenton-like reaction in a H_2O_2/schwertmannite system. Chemical Engineering Journal, 2016, 283: 873–879
6. Yang P Z, Luo S, Liu Y Z, Jiao W Z. Degradation of nitrobenzene wastewater in an acidic environment by Ti(IV)/H_2O_2/O_3 in a rotating packed bed. Environmental Science and Pollution Research International, 2018, 25: 25060–25070
7. Elshafei G M S, Yehia F Z, Dimitry O H, Badawi A M, Eshaq G. Ultrasonic assisted-Fenton-like degradation of nitrobenzene at neutral pH using nanosized oxides of Fe and Cu. Ultrasonics Sonochemistry, 2014, 21: 1358–1365
8. Wu J, Su T M, Jiang Y X, Xie X L, Qin Z Z, Ji H B. Catalytic ozonation of cinnamaldehyde to benzaldehyde over CaO: experiments and intrinsic kinetics. AIChE Journal. American Institute of Chemical Engineers, 2017, 63: 4403–4417
9. Martins R C, Cardoso M, Dantas R F, Sans C, Esplugas S, Quinta-Ferreira R M. Catalytic studies for the abatement of emerging contaminants by ozonation. Journal of Chemical Technology and Biotechnology (Oxford, Oxfordshire), 2015, 90: 1611–1618
10. Huber M M, Canonica S, Park G Y, Von Gunten U. Oxidation of pharmaceuticals during ozonation and advanced oxidation processes. Environmental Science & Technology, 2013, 37: 1016–1024
11. Sun X M, Wu C Y, Zhou Y X, Han W. Using DOM fraction method to investigate the mechanism of catalytic ozonation for real wastewater. Chemical Engineering Journal, 2019, 369: 100–108
12. Chiang Y P, Liang Y Y, Chang C N, Chao A C. Differentiating ozone direct and indirect reactions on decomposition of humic substances. Chemosphere, 2006, 65: 2395–2400
13. Beltrán F J, Encinar J M, Alonso M A. Nitroaromatic hydrocarbon ozonation in water. 1. Single ozonation. Industrial & Engineering Chemistry Research, 1998, 37: 25–31
14. Hoigné J, Bader H. Rate constants of reactions of ozone with organic and inorganic compounds in water—I: non-dissociating organic compounds. Water Research, 1983, 17(2): 173–183
15. Jiao W Z, Luo S, He Z, Liu Y Z. Applications of high gravity technologies for wastewater treatment: a review. Chemical Engineering Journal, 2017, 313: 912–927
16. Burns J R, Ramshaw C. Process intensification: visual study of liquid maldistribution in rotating packed beds. Chemical Engineering Science, 1996, 51: 1347–1352
17. Chen Y H, Chang C Y, Su W L, Chiu C Y, Yu Y H, Chiang P C, Chang C F, Shie J L, Chiou C S. Chiang S I M. Ozonation of CI Reactive Black 5 using rotating packed bed and stirred tank reactor. Journal of Chemical Technology and Biotechnology, 2015, 80: 68–75
18. Chiang C Y, Chen Y S, Liang M S, Lin F Y, Tai C Y D, Liu H S. Absorption of ethanol into water and glycerol/water solution in a rotating packed bed. Journal of the Taiwan Institute of Chemical Engineers, 2009, 40: 418–423
19. Luo Y, Chu G W, Zhou H K, Zhao Z Q, Dudukovic M P, Chen J F. Gas-liquid effective interfacial area in a rotating packed bed. Industrial & Engineering Chemistry Research, 2012, 51: 16320–16352
20. Zeng Z Q, Zhou H K, Li X, Arowo M, Sun B C, Chen J F, Chu G W, Shao L. Degradation of phenol by ozone in the presence of Fenton reagent in a rotating packed bed. Chemical Engineering Journal, 2013, 229: 404–411
21. Jiao W Z, Liu Y Z, Liu W L, Li J, Shao F, Wang C R. Degradation of nitrobenzene-containing wastewater with O_3 and H_2O_2 by high gravity technology. China Petroleum Processing and Petrochemical Technology, 2013, 15(1): 85–94
22. Guo L, Jiao W Z, Liu Y Z, Xu C C, Liu W L, Li J. Treatment of nitrobenzene-containing wastewater using different combined processes with ozone. Chinese Journal Energetic Materials, 2014, 22(5): 702–708
23. Yang P Z, Luo S, Liu H Y, Jiao W Z, Liu Y Z. Aqueous ozone decomposition kinetics in a rotating packed bed. Journal of the Taiwan Institute of Chemical Engineers, 2019, 96: 11–17
24. Jung Y, Hong E, Kwon M, Kang J W. A kinetic study of ozone decay and bromine formation in saltwater ozonation: effect of O_3 dose, salinity, pH, and temperature. Chemical Engineering Journal, 2017, 312: 30–38
25. Chu W, Ma C W. Quantitative prediction of direct and indirect dye ozonation kinetics. Water Research, 2000, 34: 3153–3160
26. Zhao Y, Yu G, Chen S Y, Zhang S Y, Wang B, Huang J, Deng S B, Wang Y J. Ozonation of antidepressant fluoxetine and its metabolite product norfluoxetine: kinetics, intermediates and toxicity. Chemical Engineering Journal, 2017, 316: 951–963
27. Chen W R, Wu C, Elovitz M S, Linden K G, Suffet I H. Reactions of thiocarbamate, triazine and urea herbicides, RDX and benzenes on EPA Contaminant Candidate List with ozone and with hydroxyl

radicals. Water Research, 2008, 42(1-2): 137–144
28. Hoigné J. Inter-calibration of ·OH radical sources and water quality parameters. Water Science and Technology, 1997, 35: 1–8
29. Leitner N K V, Roshani B. Kinetic of benzotriazole oxidation by ozone and hydroxyl radical. Water Research, 2010, 44(6): 2058–2066
30. El Najjar N H, Touffet A, Deborde M, Journel R, Leitner N K V. Levofloxacin oxidation by ozone and hydroxyl radicals: kinetic study, transformation products and toxicity. Chemosphere, 2013, 93(4): 604–611
31. Wang Z Y, Shao Y S, Gao N Y, An A. Degradation kinetic of dibutyl phthalate (DBP) by sulfate radical-and hydroxyl radical-based advanced oxidation process in UV/persulfate system. Separation and Purification Technology, 2018, 195: 92–100
32. Shen J M, Chen Z L, Xu Z Z, Li X Y, Xu B B, Qi F. Kinetics and mechanism of degradation of *p*-chloronitrobenzene in water by ozonation. Journal of Hazardous Materials, 2008, 152: 1325–1331
33. Li B Z, Xu X, Zhu L. Ozonation of chloronitrobenzenes in aqueous solution: kinetics and mechanism. Journal of Chemical Technology and Biotechnology, 2009, 84: 167–175
34. Wang F, Wang Y, Ji M. Mechanisms and kinetics models for ultrasonic waste activated sludge disintegration. Journal of Hazardous Materials, 2005, 123: 145–150
35. Ko C H, Guan C Y, Lu P J, Chern J M. Ozonation of guaiacol solution in a rotating packed bed. Chemical Engineering Journal, 2011, 171: 1045–1052
36. Zeng Z Q, Zou H K, Li X, Sun B C, Chen J F, Shao L. Ozonation of phenol with O_3/Fe(II) in acidic environment in a rotating packed bed. Industrial & Engineering Chemistry Research, 2012, 51: 10509–10516
37. Zhao W R, Wu Z B, Wang D H. Ozone direct oxidation kinetics of cationic red X-GRL in aqueous solution. Journal of Hazardous Materials, 2006, 137(3): 1859–1865
38. Zhao W R, Liu F F, Yang Y, Tan M, Zhao D Y. Ozonation of cationic red X-GRL in aqueous solution: kinetics and modeling. Journal of Hazardous Materials, 2004, 57: 1189–1199
39. Matthews R W, Sangster D F. Measurement by benzoate radiolytic decarboxylation of relative rate constants for hydroxyl radical reactions. Journal of Physical Chemistry, 1965, 69(6): 1938–1946
40. Chen Y H, Chang C Y, Su W L, Chen C C, Chiu C Y, Yu Y H, Chiang P C, Chiang S I M. Modeling ozone contacting process in a rotating packed bed. Industrial & Engineering Chemistry Research, 2004, 43(1): 228–236
41. Hoigné J, Bader H. The role of hydroxyl radical reactions in ozonation processes in aqueous solutions. Water Research, 1976, 10(5): 377–386